

## MEASUREMENTS ON A TWO-DIMENSIONAL AEROFOIL WITH HIGH-LIFT DEVICES

by

I.R.M.Moir  
DRA Farnborough

### 0 INTRODUCTION

The tests detailed in this submission were carried out by the former British Aircraft Corporation in support of the National High Lift Programme. This Programme was a collaborative project between the Royal Aerospace Establishment Farnborough (now part of the DRA) and the aircraft industry with the aim of increasing the understanding and knowledge of all aspects of high-lift systems, and to provide a fund of data which would benefit the design of future transport aircraft.

Wind-tunnel tests were carried out on four models:

- (i) A 3-D half model (RAE)
- (ii) a swept panel wing  
(HSA Hatfield)
- (iii) a quasi-2D (end-plate) model  
(BAC Weybridge)
- (iv) a 2D model (BAC Weybridge)

BAC Warton also carried out structural analyses on various leading-edge and trailing-edge devices.

The present cases are results from the 2D tests which covered investigations into two leading-edge and two trailing-edge devices. The model had a supercritical aerofoil section, a chord of 0.7635m, and was mounted between turntables in the floor and roof of the BAC 3.96m x 2.74m low-speed wind-tunnel. Two-dimensional conditions were maintained by local suction around the wing/wall junctions. Surface pressures were measured on all the components of the wing, at two spanwise stations, one near the tunnel centreline and one near the roof. These pressures were integrated to give overall lift, drag and pitching moment coefficients. A pitot/static traverse through the wake provided the total momentum deficit. Traverses perpendicular to the wing surface at various chordwise locations provided information on wake and boundary layer development and interaction. Flow visualisation was provided by tufting of the wing surfaces.

### 1 GENERAL DESCRIPTION

#### 1.1 Model name or designation

The model will be referred to as NHLP 2D.

#### 1.2 Model type and flow conditions

The model consisted of a two-dimensional wing with high-lift devices, designed for testing at low subsonic speeds.

#### 1.3 Design requirements and purpose of tests

The model was designed for tests on a wide range of high-lift devices. The position and deflection angle of these could be varied. Two-dimensional flow conditions were maintained during tests by the use of local suction at the wing/wall junctions.

#### 1.4 Dominant flow physics

The performance of a high-lift wing is dependent upon a strong interaction between the wakes and boundary layers associated with each element (e.g. slat/wing/flap etc.). Each downstream element enables the element ahead of it to carry a higher load than it would in isolation, due to the fact that its trailing-edge is situated in the suction field of the downstream element; this makes the pressure at the trailing-edge significantly negative, so that, for a given pressure recovery, higher peak suction can be sustained. At the same time, the wake from the upstream element can interact with the boundary layer on the downstream element, thickening the latter and producing earlier separation. The former effect demands that the two elements be moved closer together, while the latter requires the two to be separated. This leads to the concept of optimum relative positions of the elements of a high-lift aerofoil. These mechanisms are illustrated in Fig 1 which shows typical pressure distributions on a three element aerofoil, together with wake/boundary layer profiles and development, derived from these profiles. Also shown is a typical plot of lift coefficient against angle of incidence which illustrates the variation of  $C_L$  with slat position.

#### 1.5 Additional remarks

The data offered here were gathered in the early 1970's, before CFD methods attained accuracy sufficient to make the comparison between theory and experiment of significance throughout the whole flow-field. Unfortunately the data presented here consist only of

surface pressures on the model and measurements of static and total head variation through the wake and boundary layers at selected chordwise positions. Despite this, the data form an unusually wide coverage of different slotted high-lift systems at moderately high Reynolds Number in a flow with an exceptionally high degree of 2-dimensionality.

The technique of using wall suction, not only to prevent the separation of side-wall boundary layers, but also to reduce their growth substantially, has been proved in a number of previous experiments<sup>1,2,3</sup>, and leads to a flow which is closely 2-dimensional. Since accurate data of this type, with highly deflected flaps, are difficult and expensive to obtain, this set should afford a valuable addition to the library of test cases available to AGARD countries.

## 2 DETAILS OF MODEL

### 2.1 General geometric arrangement

Fig 2a shows the NHLP 2D model planform, and a typical aerofoil cross-section.

### 2.2 Configurations

Fig 2b shows the alternative high-lift devices tested.

### 2.3 Wing and aerofoil data.

#### 2.3.1 Planform

Span	= 2.743m
Aspect ratio	= 3.593
Area	= 2.094m

#### 2.3.2 Basic aerofoil section

Wing section:	BAC 3-11/RES/30/21
Thickness/chord	= 11%
Nose radius r/c	= 0.0137

### 2.7 Geometric definition

The aerofoil profile was numerically defined, and the design ordinates are provided. Tolerance on the profile is  $\pm 0.13$ mm. Roughness data are not available.

### 2.8 Model support details

The model was mounted between turntables in the floor and roof of the tunnel, as shown in Fig 2a.

#### 2.8.2 Special features of mounting

Local suction was applied around the wing roots as shown in Fig 2c.

## 3 GENERAL TUNNEL INFORMATION

### 3.1 Tunnel designation

BAC Weybridge 3.96m x 2.74m

### 3.2 Organisation running tunnel:

British Aircraft Corporation(BAC)

### 3.3 Type of tunnel

Low-Speed, closed circuit.

Operating envelope: 12.2m/sec  $\rightarrow$  97.5m/sec

Maximum Re/m =  $6.6 \times 10^6$

### 3.4 Test Section

#### 3.4.1 Test section details

Fig 3 shows the model in the tunnel working section.

#### 3.4.2 Test section dimensions

3.96m x 2.74m x 6.35m

Corner fillet size: 0.762m x 0.762m approx.

#### 3.4.3 Wall geometry details

Walls of working section were solid.

No wall static pressures were measured.

Boundary layer control was applied in the region of the wing roots only.

Wall boundary layer total thickness was 88mm and displacement thickness was 10.5mm approximately.

### 3.5 Freestream conditions

#### 3.5.1 Reference pressure measurement

Total pressure was measured by a tapping in the maximum section.

Static pressure was measured by a tapping at the position shown in Fig 3. Positional corrections were applied to these readings.

Static temperature was not measured.

#### 3.5.2 Tunnel calibration

The tunnel was calibrated over three transverse planes *within the working section in the region of the model*, at a wind velocity of 30.5m/sec. A pitot-static tube with an ellipsoidal head was traversed over a grid with intervals 0.304m horizontally and 0.152m vertically. The tunnel was last calibrated in about 1969.

surface pressures on the model and measurements of static and total head variation through the wake and boundary layers at selected chordwise positions. Despite this, the data form an unusually wide coverage of different slotted high-lift systems at moderately high Reynolds Number in a flow with an exceptionally high degree of 2-dimensionality.

The technique of using wall suction, not only to prevent the separation of side-wall boundary layers, but also to reduce their growth substantially, has been proved in a number of previous experiments<sup>1,2,3</sup>, and leads to a flow which is closely 2-dimensional. Since accurate data of this type, with highly deflected flaps, are difficult and expensive to obtain, this set should afford a valuable addition to the library of test cases available to AGARD countries.

## 2 DETAILS OF MODEL

### 2.1 General geometric arrangement

Fig 2a shows the NHLP 2D model planform, and a typical aerofoil cross-section.

### 2.2 Configurations

Fig 2b shows the alternative high-lift devices tested.

### 2.3 Wing and aerofoil data.

#### 2.3.1 Planform

Span	= 2.743m
Aspect ratio	= 3.593
Area	= 2.094m

#### 2.3.2 Basic aerofoil section

Wing section:	BAC 3-11/RES/30/21
Thickness/chord	= 11%
Nose radius r/c	= 0.0137

### 2.7 Geometric definition

The aerofoil profile was numerically defined, and the design ordinates are provided. Tolerance on the profile is  $\pm 0.13$ mm. Roughness data are not available.

### 2.8 Model support details

The model was mounted between turntables in the floor and roof of the tunnel, as shown in Fig 2a.

#### 2.8.2 Special features of mounting

Local suction was applied around the wing roots as shown in Fig 2c.

## 3 GENERAL TUNNEL INFORMATION

### 3.1 Tunnel designation

BAC Weybridge 3.96m x 2.74m

### 3.2 Organisation running tunnel:

British Aircraft Corporation(BAC)

### 3.3 Type of tunnel

Low-Speed, closed circuit.  
Operating envelope: 12.2m/sec  $\rightarrow$  97.5m/sec  
Maximum Re/m =  $6.6 \times 10^6$

### 3.4 Test Section

#### 3.4.1 Test section details

Fig 3 shows the model in the tunnel working section.

#### 3.4.2 Test section dimensions

3.96m x 2.74m x 6.35m  
Corner fillet size: 0.762m x 0.762m approx.

#### 3.4.3 Wall geometry details

Walls of working section were solid.  
No wall static pressures were measured.  
Boundary layer control was applied in the region of the wing roots only.  
Wall boundary layer total thickness was 88mm and displacement thickness was 10.5mm approximately.

### 3.5 Freestream conditions

#### 3.5.1 Reference pressure measurement

Total pressure was measured by a tapping in the maximum section.  
Static pressure was measured by a tapping at the position shown in Fig 3. Positional corrections were applied to these readings.  
Static temperature was not measured.

#### 3.5.2 Tunnel calibration

The tunnel was calibrated over three transverse planes within the working section in the region of the model, at a wind velocity of 30.5m/sec. A pitot-static tube with an ellipsoidal head was traversed over a grid with intervals 0.304m horizontally and 0.152m vertically. The tunnel was last calibrated in about 1969.

### 3.6 Flow Quality of empty tunnel

#### 3.6.1 Flow uniformity

The static pressure varied approximately 0.4% over the model chord, and insignificantly across the span. The Mach number was held constant during a run. The flow angularity was measured by a pitch meter. The upwash at the model station was 0.23°. Sidewash is not available.

#### 3.6.2 Temperature variation

The tunnel temperature could not be controlled and varied approximately 5°C during a run. The variation within the tunnel is not available.

#### 3.6.3 Flow unsteadiness

The tunnel turbulence factor was 1.068. The noise level is not available.

## 4 INSTRUMENTATION

### 4.1 Model position

#### 4.1.1 Measurement of geometrical incidence

The geometrical incidence was derived from the rotation angle of the turntables.

#### 4.1.2 Accuracy of incidence measurement = ±0.05°.

### 4.2 Model pressure measurement

#### 4.2.1 Number and disposition of pressure tappings

Fig 4a indicates the position of the pressure tappings on the components of the model. Tappings are located at two spanwise stations as shown in Fig 2a.

#### 4.2.2 Range of pressure transducers

Statham unbonded strain-gauge type pressure transducers were used with ranges matched to the expected pressures on the wing. 34.5kPa, 17.2kPa, 6.9kPa and 3.4kPa ranges were used.

#### 4.2.3 Dynamic pressures were not measured.

### 4.3 Force and moment measurement

#### 4.3.1 Type of balance

No balance was used as sectional force and moment coefficients were obtained from integration of the pressure coefficients.

### 4.4 Boundary layer and flow field measurements

4.4.1/2/3 Boundary layer measurements were made by traversing a pitot/static probe normal to the wing surface. Wake momentum deficit was measured by a pitot/static rake mounted downstream of the model on a traversing rig which enabled it to be aligned with the model wake, as shown in Fig 4b.

### 4.5 Surface flow visualisation.

4.5.1/2 Surface flow visualisation was carried out by means of wool tufts attached to the surface at various locations on the wing and leading and trailing edges.

#### 4.5.3 Results of flow visualisation

These are in the form of photographs, but cannot be made available.

## 5 TEST MATRIX AND CONDITIONS

### 5.1 Detailed test matrix

#### 5.1.1 Number of selected test cases

Eight test cases are offered, consisting of surface pressure measurements and boundary layer traverses at two angles of incidence for one configuration, and at three angles of incidence for two other configurations. Note that not all boundary layer traverse positions are covered at each angle of incidence. The configurations offered are listed in 5.1.2.

#### 5.1.2 Configurations tested

The configurations tested were:

- (i) L1 slat (12.5%) at 25° + T2 single-slotted flap at 20°
- (ii) L1 slat + T7 double-slotted flap at 40°
- (iii) L1 slat + T8 triple-slotted flap(7.5°,40°,20°)

#### 5.1.3 Test matrix

A full test matrix is given in Table 1.

### 5.2 Model/tunnel relations

#### 5.2.1 Maximum blockage

Maximum solid blockage =  $\Delta U/U_0 = 0.00169$

#### 5.2.2 Model span/tunnel width = 1

#### 5.2.3 Wing area/tunnel cross section

S/C = 0.215 approx (area of fillets has been estimated)

**5.2.4** Tunnel height/chord ratio = 3.593

**5.2.5** Tunnel width/chord ratio = 5.190

### **5.3** Transition details

**5.3.1** Transition was fixed on the wing upper and lower surfaces.

**5.3.2** At high-lift the upper surface transition was forward of the transition fix due to a short laminar bubble near the leading-edge.

**5.3.3** Details of the transition fixing is shown in Fig 5. No data are available on the effectiveness of the fixing, apart from as stated in 5.3.2.

## **6** DATA

### **6.1** Availability of data

#### **6.1.1** Organisation owning the data

Defence Research Agency, Farnborough

#### **6.1.2** Person responsible for the data

Dr D.S.Woodward,  
Superintendent AP3 Division,  
Aerodynamics & Propulsion Dept.,  
X80 Building,  
Defence Research Agency,  
Farnborough,  
Hampshire GU14 6TD  
United Kingdom  
Tel: 0252-395377  
Fax: 0252-377783

#### **6.1.3** Availability of data

The data specified in this document are freely available.

### **6.2** Suitability of data for CFD validation.

**6.2.1** Data are suitable for 'in tunnel' calculation, although no wall pressure data are available. Data are corrected for solid blockage, and by a simple correction to incidence to represent the effect of wall constraint as follows:

$$\Delta\alpha = 0.0693(C_L + 4C_m)^\circ$$

No camber or wake blockage corrections have been applied, but full incidence polars will be supplied for the calculation of these quantities.

**6.2.2** Data are corrected to simulate 'free-air' conditions.

### **6.3** Type and form in which data are available.

**6.3.1** Details are given in Table 2 of the form in which the various components of the data exist.

Freestream velocity is corrected for solid blockage.

Pressure coefficients are based of freestream dynamic pressure, corrected for solid blockage.

Force and moment coefficients are based on corrected freestream dynamic pressure, and are also corrected for wall constraint, as detailed in 6.2.1.

**6.3.2** At the time of the preparation of this document the data were only available in printed form, but were being prepared for availability on floppy disk.

#### **6.3.3/4** Extent of data

This was not available at the time of preparation of this document.

### **6.4** Corrections applied to data.

#### **6.4.1** Lift interference and blockage correction

The data are considered to be globally correctable. Classical correction methods are applied according to Ref 4.

Dynamic pressure, angle of incidence, and pressure coefficients are corrected. Some uncorrected data may be available.

#### **6.4.2** Side wall interference corrections

The wall boundary layer was removed by suction in the region of the model.

#### **6.4.5** Aeroelastic deformation

This was not measured as the model itself was rigidly mounted and the high-lift devices were mounted on 10 brackets which minimised deformation.

**6.4.6** It is not known if corrections were made for effect of wake traverse, etc. No measurements were made to determine the effect of bracket wake on the flow.

## **7** DATA ACCURACY AND REPEATABILITY ASSESSMENT

### **7.1** Accuracy estimates

#### **7.1.1** Free-stream conditions

Mach number -  $\pm 0.5\%$

Flow velocity - as Mach No

Angle of incidence -  $\pm 0.05^\circ$

### 7.1.2 Measured data

Forces and moments -

$C_N$   $\pm 0.12\%$

$C_A$   $\pm 0.2\%$

$C_m$   $\pm 0.15\%$

Pressure coefficients -  $\pm 0.1\%$

### 7.2 Repeat measurements.

#### 7.2.1 Type and number of repeats during one test series

Unknown

#### 7.2.2 Type and number of repeats in successive tests

Unknown

### 7.4 Other tests on the same nominal geometry.

7.4.1 The model was not tested in any other tunnel.

7.4.2 Related models have been tested in other tunnels - see Introduction.

## 8 REFERENCES

1. D.N.Foster      The Two-Dimensional Flow  
H.P.A.H.Irwin    around a Slotted Flap.  
B.R.Williams    R&M 3681 1971
2. I.R.M.Maar      The Measurement and  
D.N.Foster      Analysis of the  
D.R.Holt        Profile Drag of a Wing with  
                    Slotted Flap.  
                    RAE TR 71158 1971
3. D.N.Foster      The nature, development, and  
P.R.Ashill      effect of the Viscous Flow  
B.R.Williams    around an Aerofoil with High  
                    Lift Devices.  
                    RAE TR 72227 1972
4. H.C.Garner      Subsonic Wind Tunnel  
E.W.E.Rogers    Corrections  
W.E.A.Acum      AGARDOGRAPH 109  
E.C.Maskell      October 1966

TABLE 1

Case No.	Slat	Flap	$U_0$ m/s	$q$ kPa	$Re$ $\times 10^{-6}$	Notes
1	L1	T2	67.0	2.75	3.52	Optimum slat position. Boundary layer traverse at $\alpha = 4^\circ$ , at 25% wing chord, shroud t/e, 50% flap chord, flap t/e.
2	L1	T2	67.0	2.75	3.52	Optimum slat position. Boundary layer traverse at $\alpha = 20^\circ$ , at 25% wing chord, shroud t/e, 50% flap chord, flap t/e.
3	L1	T7	54.9	1.85	2.88	Boundary layer traverses at $\alpha = 3^\circ$ , at 37.2% wing chord, aft of flap trailing edge.
4	L1	T7	54.9	1.85	2.88	Boundary layer traverses at $\alpha = 17^\circ$ , at 37.2%, 80%, 91% wing chord, 50% vane chord, 50%, 75% flap, aft of flap trailing edge.
5	L1	T7	54.9	1.85	2.88	Boundary layer traverses at $\alpha = 19^\circ$ , at 37.2%, 80%, 91% wing chord, 50% vane chord, 50%, 75% flap, aft of flap trailing edge.
6	L1	T8	54.9	1.85	2.88	Boundary layer traverse at $\alpha = 3^\circ$ , aft of flap trailing edge.
7	L1	T8	54.9	1.85	2.88	Boundary layer traverse at $\alpha = 15^\circ$ , aft of wing shroud t/e, flap shroud t/e, flap t/e.
8	L1	T8	54.9	1.85	2.88	Boundary layer traverse at $\alpha = 17^\circ$ , aft of wing shroud t/e, flap shroud t/e, flap t/e.

Notes: Surface pressures measured and wake traverse for all cases.  
 $Re$  is based on retracted chord of 0.7635m.

TABLE 2

Data	Engineering Units	Coefficients	Normalised	Uncorrected	Corrected
Freestream Conditions	Yes	-	-	-	Yes
Surface Pressures	No	Yes	No	No	Yes
Forces	No	Yes	No	Yes	Yes
b/l Data	Yes	Yes	No	No	Yes
Wake Data	Yes	Yes	No	No	Yes

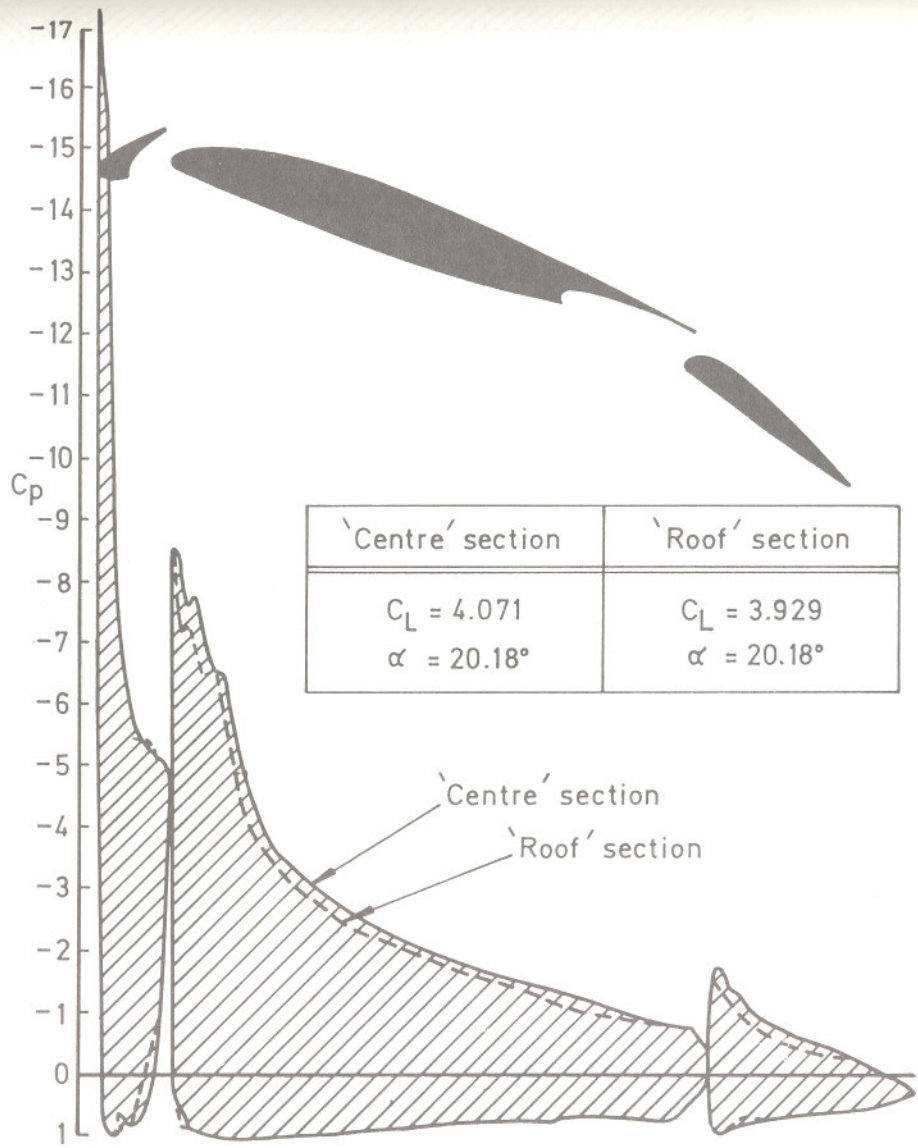


Fig 1a Typical pressure distribution on three element high-lift aerofoil

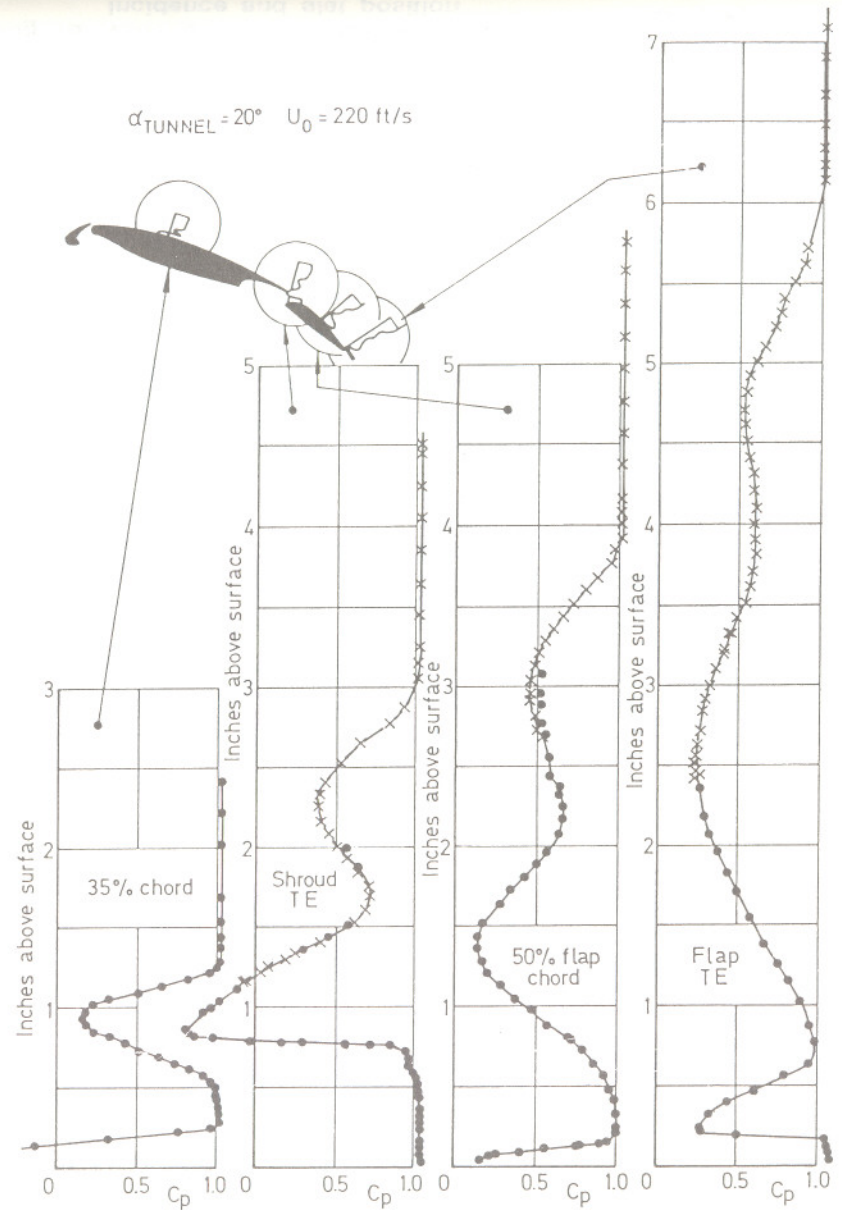


Fig 1b Typical wake/boundary layer velocity profiles



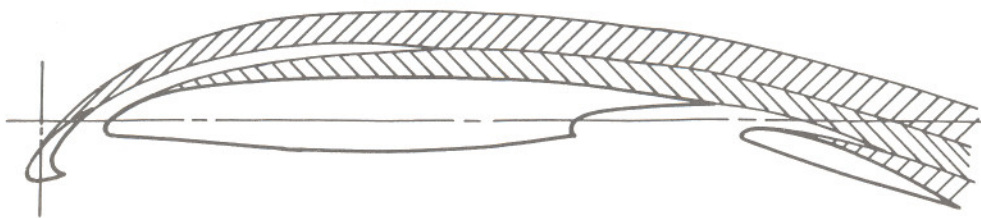


Fig 1c Wake/boundary layer interaction on three element high-lift aerofoil

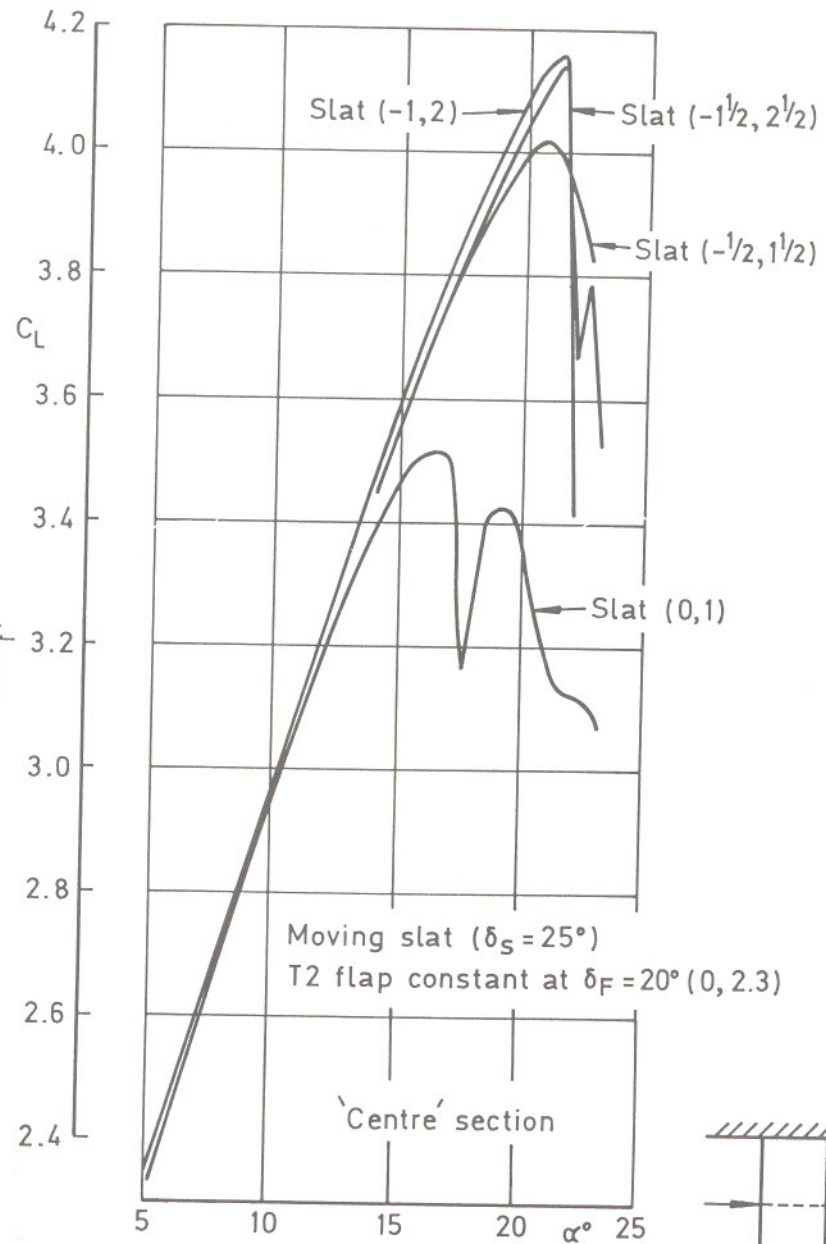
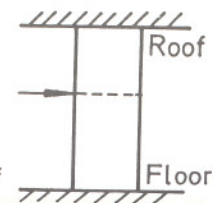


Fig 1d Variation of lift coefficient with angle of incidence and slat position



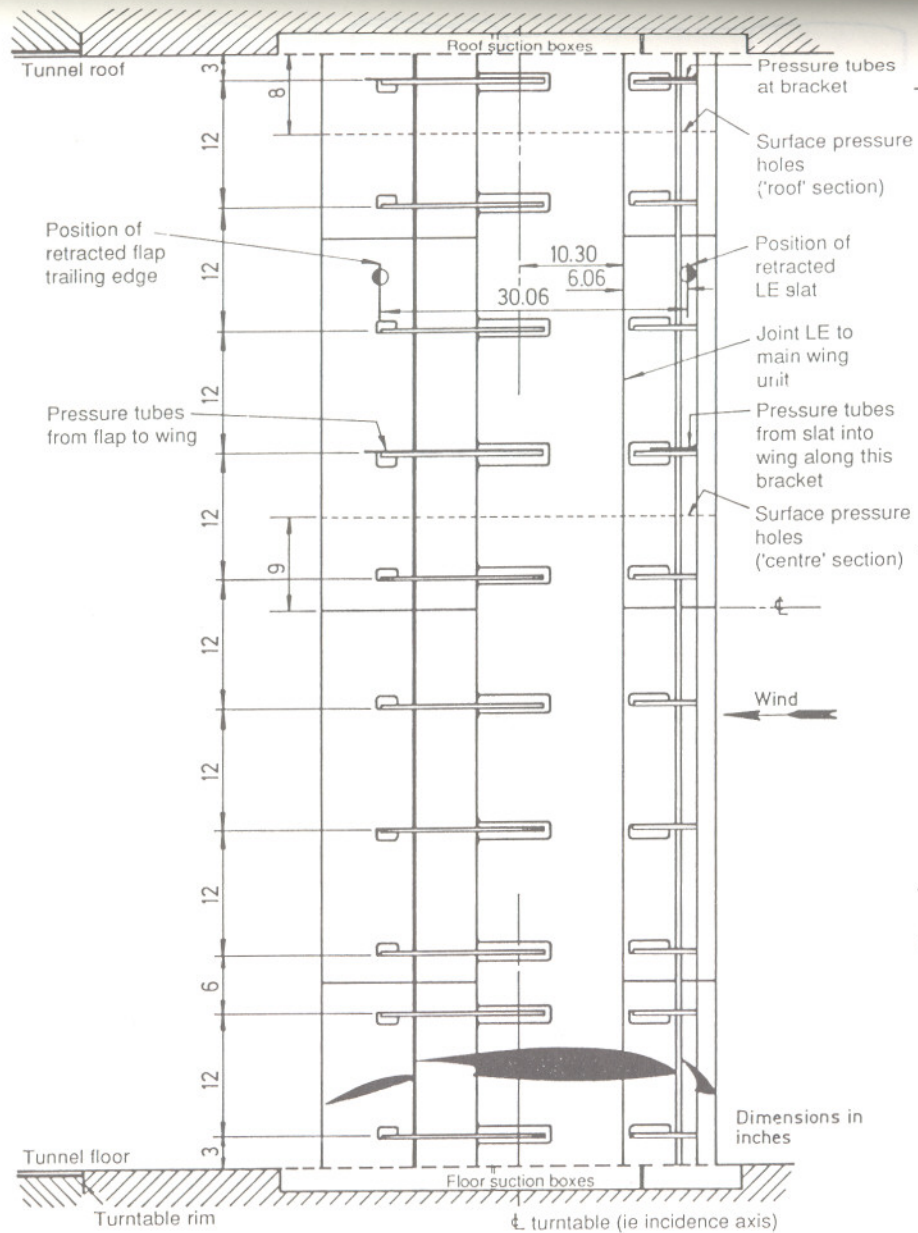


Fig 2a NHLP 2D model planform

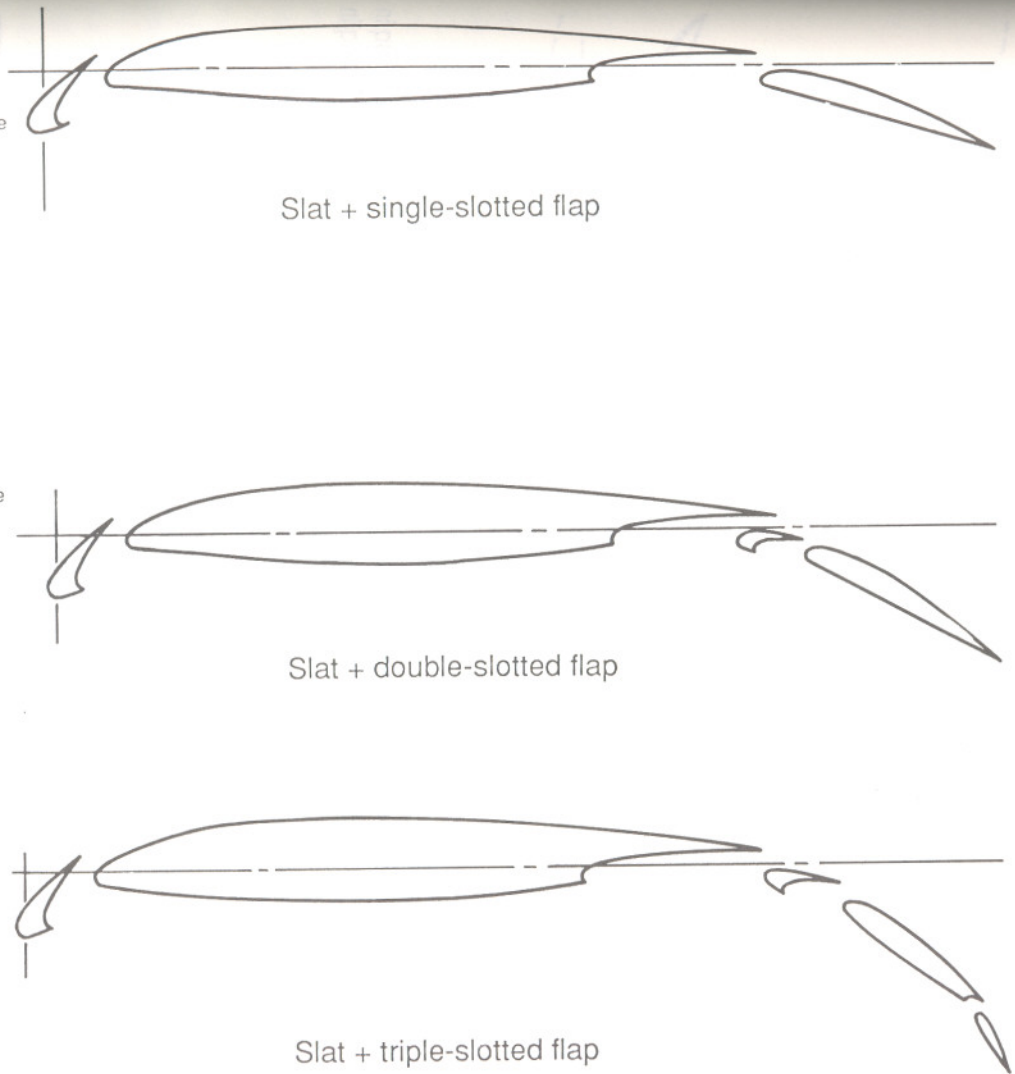
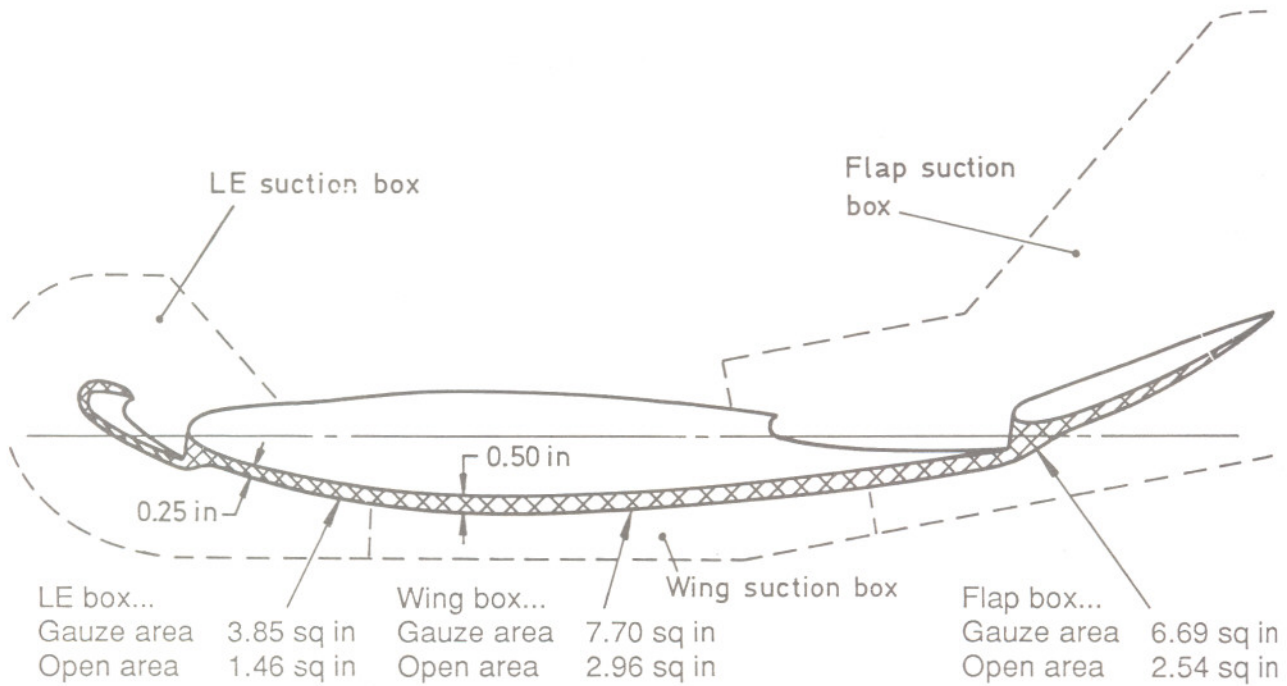


Fig 2b Alternative configurations



The porous area of each box is sealed by cover plates and tape to leave only the open strip along profile upper surface as shown in sketch

Fig 2c Distribution of suction areas around wing at roof and floor of tunnel

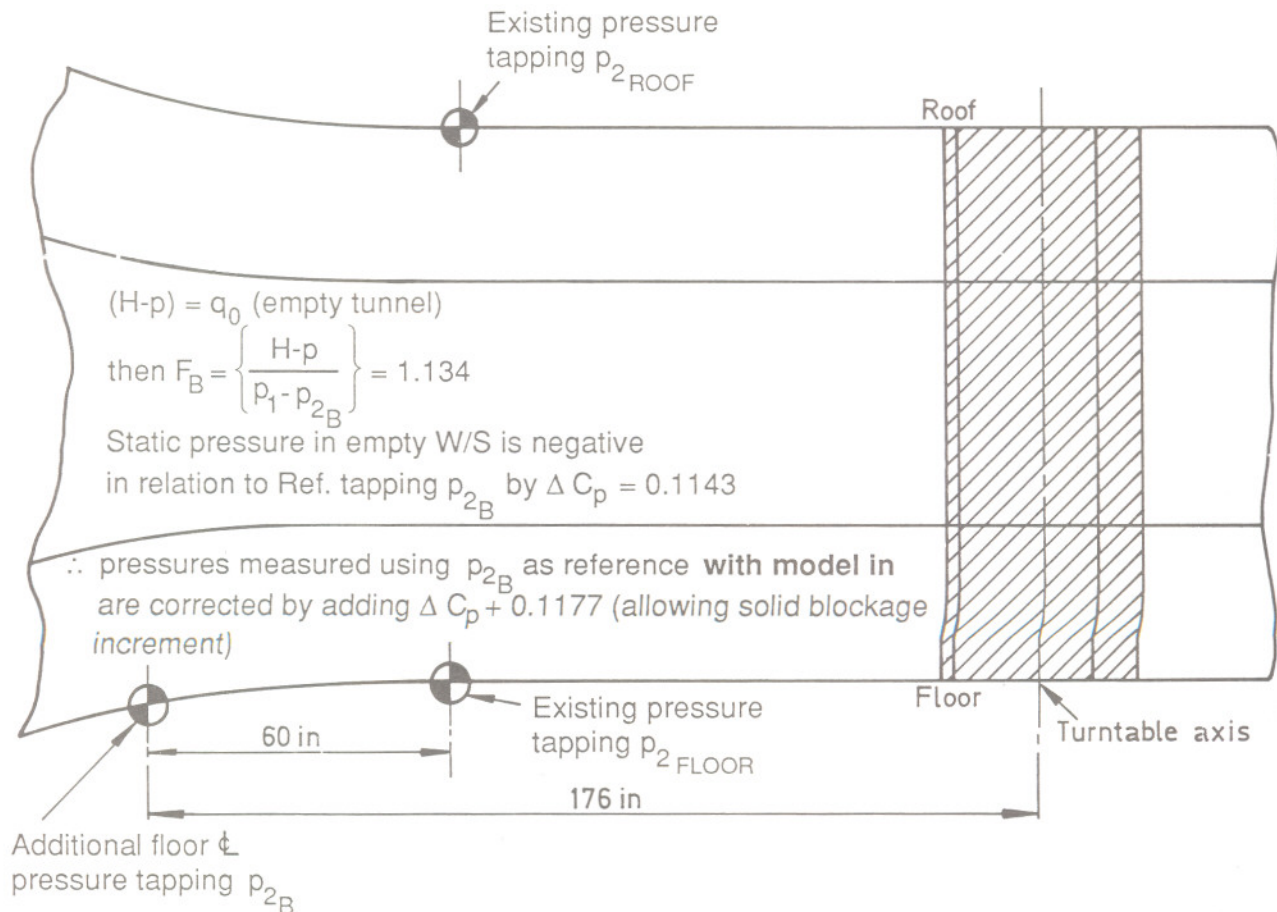


Fig 3 NHLP 2D model in tunnel, showing reference pressure tapings

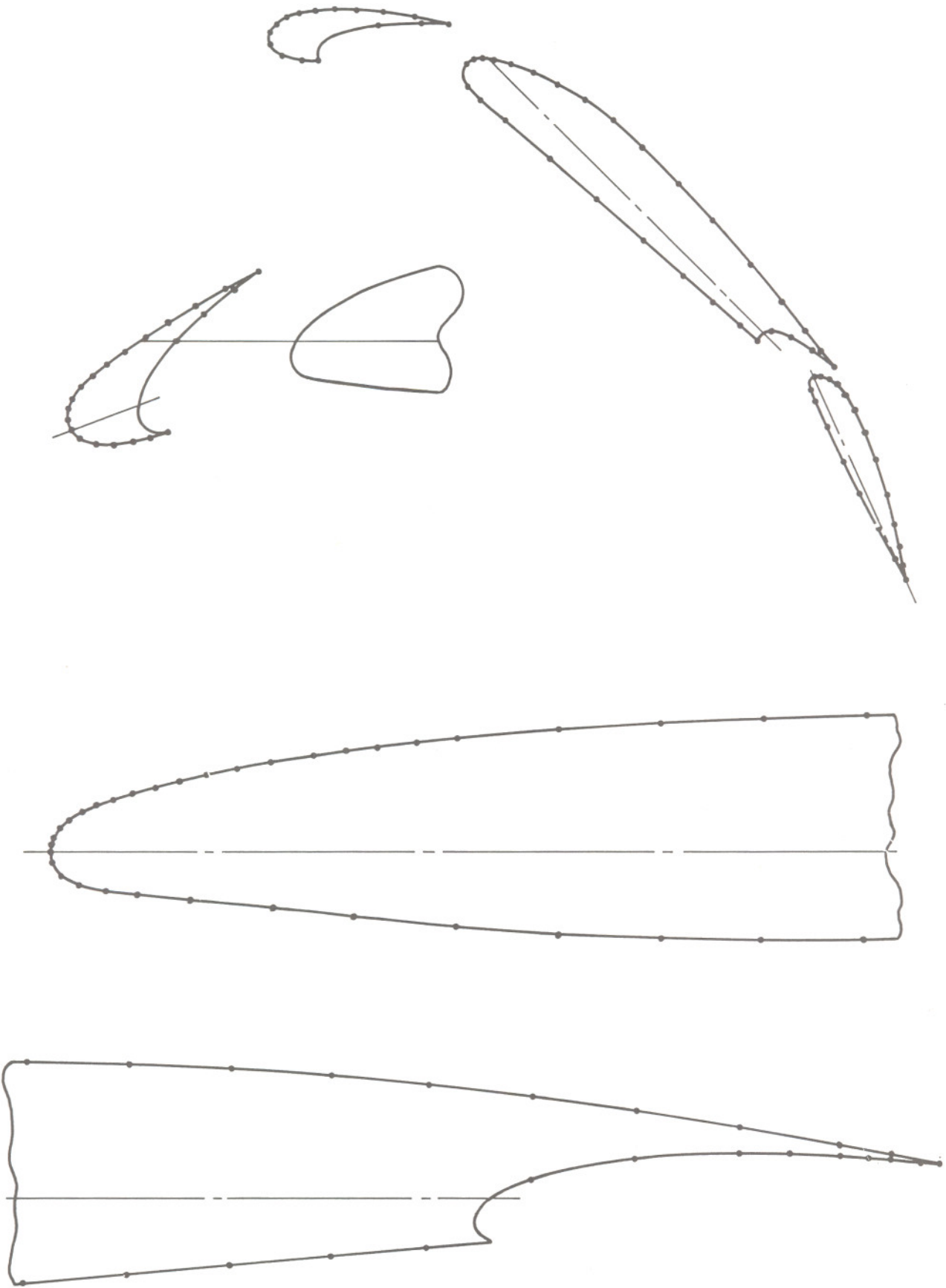
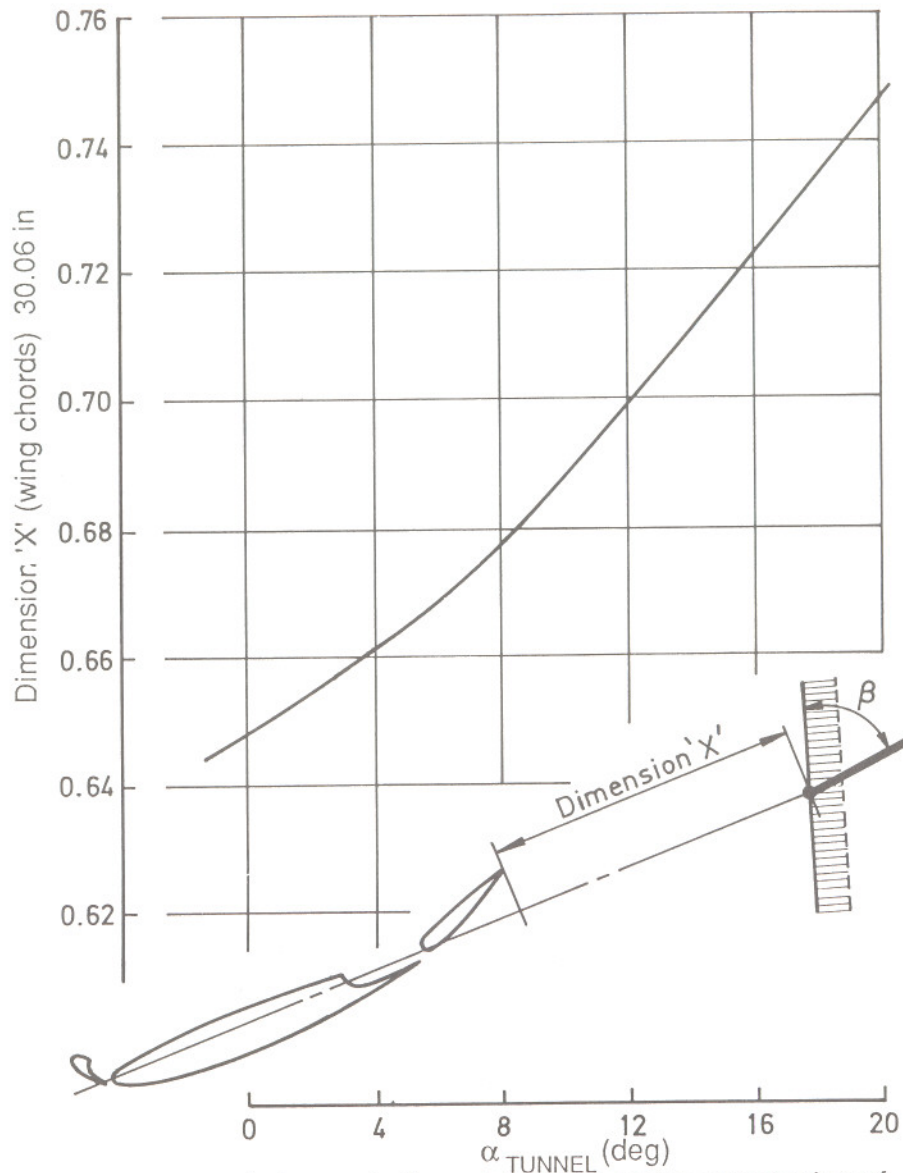


Fig 4a Positions of pressure tappings on wing surface



(rake angle  $\beta$  predetermined from observation of cotton streamer attached to rake)  
 Fig 4b Position of wake rake relative to model

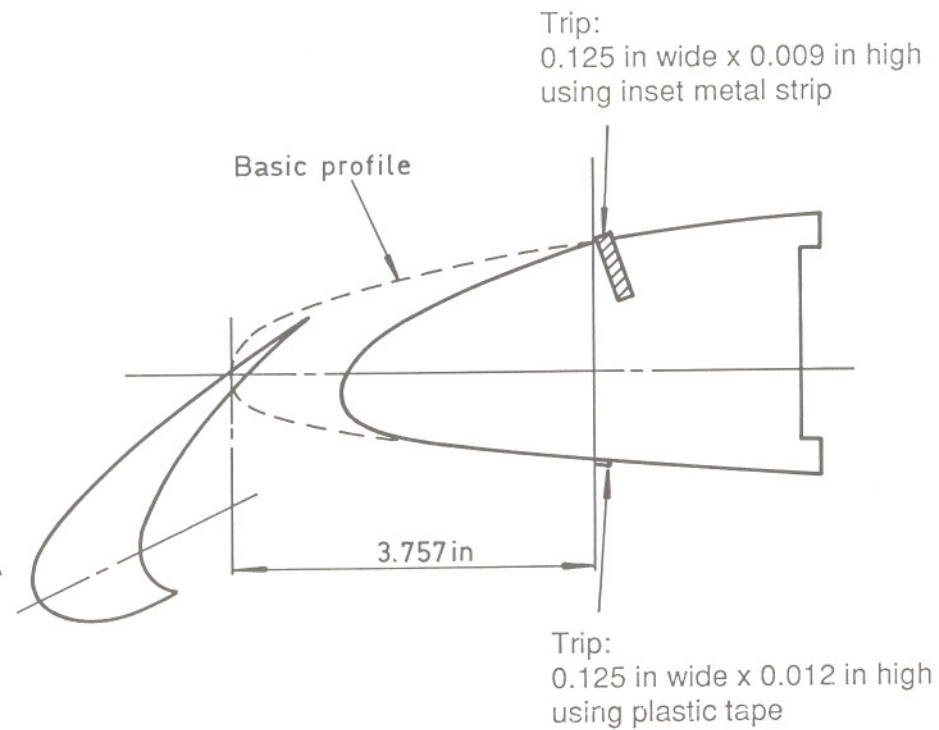


Fig 5 Details of transition fix